CIENCIA 15(2), 234 - 241, 2007
Maracaibo, Venezuela

Optical properties of $Cu(In_{1-x}Ga_x)_5Se_8$ from ellipsometric measurements*

*Larissa Durán[1]**, Jaime Castro[1], Elvis Hernández[1], Ángel Muñoz[2], José Naranjo[3] and Carlos Alberto Durante Rincón[1]*

[1]*Laboratorio de Ciencia de Materiales, Departamento de Física, Facultad Experimental. de Ciencias, Universidad del Zulia, Apartado Postal 526, Maracaibo, Venezuela.* [2]*Laboratorio de Astronomía y Física Teórica (LAFT). Departamento de Física. Facultad Experimental de Ciencias, Universidad del Zulia, Maracaibo, Venezuela.* [3]*Instituto Universitario de Tecnología de Maracaibo. Maracaibo, Venezuela.*

Recibido: 30-11-05 Ac eptado: 10-04-06

Abstract

Spectroscopic ellipsometry measurements at room temperature were done on the system $Cu(In_{1-x}Ga_x)_5Se_8$ This allowed to determine the real and imaginary parts of the complex refractive index N(hν), the real and imaginary parts of the complex dielectric function ε(hν), the absorption coefficient α(hν) and the reflectivity R(hν) for each studied composition. The value of the energy gap E_g for each composition was obtained from fitting the numerically obtained second derivative spectra of the experimental data ε(hν), $d^2\varepsilon(h\nu)/d(h\nu)^2$, to analytic critical-point line shapes. The energy gap values of $CuIn_5Se_8$ and $CuGa_5Se_8$, thus obtained, are in good agreement with those reported by other authors. The value of the high frequency dielectric constant ε_∞ for each composition was determined fitting the real refractive index n to the Sellmeier dispersion formula.

Key words: Ellipsometry; optical properties; ordered vacancy semiconductors.

Propiedades opticas de $Cu(In_{1-x}Ga_x)_5Se_8$ a partir de medidas elipsométricas

Resumen

Medidas de elipsometría espectroscópica a temperatura ambiente se llevaron a cabo sobre el sistema $Cu(In_{1-x}Ga_x)_5Se_8$. Esto permitió determinar las partes real e imaginaria del índice de refracción complejo N(hν), las partes real e imaginaria de de la función dieléctrica compleja ε(hν), el coeficiente de absorción α(hν) y la reflectividad R(hν) para cada composición estudiada. El valor de la brecha de energía E_g para cada composición se obtuvo ajustando los espectros de la segunda derivada de la data experimental ε(hν), $d^2\varepsilon(h\nu)/d(h\nu)^2$, numéricamente obtenidos, a curvas analíticas con puntos críticos. Los valores de la brecha de energía de $CuIn_5Se_8$ y $CuGa_5Se_8$, así calculados, están en buen acuerdo con los reportados por otros autores. El valor de la constante dieléctrica de alta frecuencia ε_∞ se obtuvo para cada composición ajustando el índice de refracción real n a la formula de dispersión de Sellmeier.

Palabras clave: Elipsometría; propiedades ópticas; semiconductores con vacantes ordenadas.

* Trabajo presentado en el V Congreso de la Sociedad Venezolana de Física, Universidad del Zulia. Nucleo Punto Fijo - Edo. Falcón, Venezuela, Noviembre 2005.

** Autor para la correspondencia. Tel.: + 58-261-7598160. E-mail: durin@cantv.net

Introduction

Information about spectral dependence of optical parameters such as dielectric constant, refractive index, reflectivity and absorption coefficient are essential in the characterization of materials that are used in the fabrication of opto-electronic devices and also in the optimization of the efficiency of thin films solar cells. One of the non-destructive techniques that are being employed lately for the optical characterization is spectroscopic ellipsometry (SE) (1-4).

The SE (5, 6) is an excellent technique for measuring dielectric functions, since these can be obtained without the need of Kramers-Kronig transformations. This technique measures the change in the polarization state of the light reflected from the sample's surface. In addition, its high surface sensitivity allows surface conditions to be assessed and optimized in real time.

The complex dielectric function $\varepsilon = \varepsilon_r - j\varepsilon_i$ of the sample, where ε_r and ε_i are the real and imaginary parts, is calculated from the ellipsometric data using the isotropic two-phase model that involves the medium and the sample (1). ε is related to the complex refractive index N through the relation $\varepsilon = N^2 = (n - jk)^2$. In this relation, n is the real part of the refractive index and k the extinction coefficient. These parameters can be determined by solving the following equations:

$$\varepsilon_r = n^2 - k^2 \quad [1]$$

$$\varepsilon_i = 2nk \quad [2]$$

The optical absorption coefficient α and the normal incidence reflectivity R can be calculated through the relations:

$$\alpha = \frac{4\pi k}{\lambda} \quad [3]$$

$$R = \frac{(n-1)^2 + k^2}{(n+1)^2 + k^2} \quad [4]$$

To our knowledge no SE data is available on $Cu(In_{1-x}Ga_x)_5Se_8$ alloys, even though optical studies have been performed earlier (7-10). In the present work, using SE, we report on the spectral dependence at room temperature, in the energy range between 0.7 and 5.2 eV, of the absorption coefficient, the complex dielectric function, the complex refractive index, the reflectivity and the high frequency dielectric constant of $Cu(In_{1-x}Ga_x)_5Se_8$ alloys.

Experimental Methods

Ingots of $Cu(In_{1-x}Ga_x)_5Se_8$ alloys with x=0, 0.2, 0.4, 0.6, 0.8 and 1.0 were prepared by direct fusion of the stoichiometric mixture of constituent elements of at least 5N purity in evacuated quartz ampoules. These were previously coated with carbon. Details related to the crystal growth have been reported earlier (7, 8). The composition of each resultant alloy was determined by atomic emission spectroscopy performed on HNO_3 solutions of the samples using an ICP Perkin Elmer Optima 3200 RL. As shown in Table 1, this was close to the ideal theoretical value of the starting composition. As observed by a thermal probe, samples cut from the ingots showed n-type conductivity for $x \leq 0.4$ and p-type for $x \geq 0.6$. The unit cell parameters a and c for different composition x, obtained from the analysis of x-ray powder diffraction data using a Siemens D5005 diffractometer with copper anode and Bragg-Brentano geometry, are also given in Table 1. These data further confirm that a single phase with tetragonal structure occurs for $x \geq 0.4$, whereas for $x < 0.4$, tetragonal and hexagonal phases coexist below about 850°C (7).

Ellipsometric measurements were made, using a spectral ellipsometer SOPRA ES4G equipped with rotating polarizer, on samples that had surface area of about 4 mm^2 and thickness of around 1 mm. To minimize the contribution to the experimental data of thin films of oxide that are formed on the sample surface due to oxidation and also to reduce the effect of surface rough-

Table 1
Stoichiometric composition and unit cell lattice parameters of Cu(In1-xGax)5Se8 alloys.

	Cu	In	Ga	Se	*a*(Å)	*c*(Å)
$CuIn_5Se_8$	0.7	4.7	-	7.6	5.718(5) 4.030(1)[h]	11.62(3) 16.372(1)[h]
$Cu(In_{0.8}Ga_{0.2})_5Se_8$	0.6	3.9	0.8	7.6	5.6909(8)	11.3988(3)
$Cu(In_{0.6}Ga_{0.4})_5Se_8$	0.8	3.0	1.6	7.5	5.6384(9)	11.2745(9)
$Cu(In_{0.4}Ga_{0.6})_5Se_8$	1.1	1.5	3.1	7.6	5.5809(4)	11.1336(7)
$Cu(In_{0.2}Ga_{0.8})_5Se_8$	1.0	0.6	4.0	7.7	5.5262(7)	11.0361(7)
$CuGa_5Se_8$	1.0	–	4.6	8.0	5.4810(4)	10.937(1)

Values in the parenthesis indicate standard deviation in the last digit.
[h]hexagonal structure, γ= 120°.

ness to which ellipsometry is very sensitive, the samples were polished to attain optical quality just before acquiring ellipsometric data. The focused light spot on the sample surface allowed locating the adequate point to achieve the best response.

Results and Discussion

The variation of the refractive index *n* and the extinction coefficient *k* as functions of wavelength for the $Cu(In_{1-x}Ga_x)_5Se_8$ samples are shown in Figures 1 and 2, respectively. We observed that the real index spectra have an overall similar behavior. This is also valid for the imaginary index spectra. In the spectral region of low absorption, accuracy of measurements with the used ellipsometer (without a compensator) is known to be rather poor [1, 3]: we consider that measured values of $k<0.1$ are too imprecise and inaccurate. It is worth emphasizing that the measured values of *n* are not affected by this problem.

In Figure 2, it is significant that all samples display, in higher or lower degree, absorption tails below the fundamental gap edge. These tails result from several causes. Besides intrinsic contributions such as alloy disorder, other causes such as grain boundaries in polycrystalline material and deviation from stoichiometry can give rise to such tails (1).

From *n* and *k*, optical magnitudes of interest are calculated easily. The absorption coefficient and the normal-incidence R were calculated using the relations [3] and [4]. As in other alloy systems (1, 3) the dependence of the refraction index on composition at a fixed energy below the band gap is a smooth curve. While *n* is quite dependent on surface preparation, the value of R is much less sensitive to thin over-layers and is thus a helpful quantity for characterization purposes. A suitable working energy in the present case is that of the near-infrared (IR) He-Ne laser line, λ = 1.523 μm (0.814 eV). The values R(x) calculated from our data are given in Figura 3. Our data are well represented by the best-fit parabola.

$$R = 0.22359 - 0.02603x + 0.01072x^2 \quad (0.97) \qquad [5]$$

The good fit implies that this is a valid method to evaluate the composition of these alloys. However, it is important to reveal that values of *R* to x= 0.4 and 0.8 could not been fitted, cause in the low energy range present an untypical behavior, showing a slide deviation due to superficial problems.

The dielectric function of a semiconductor is closely linked to its electronic band

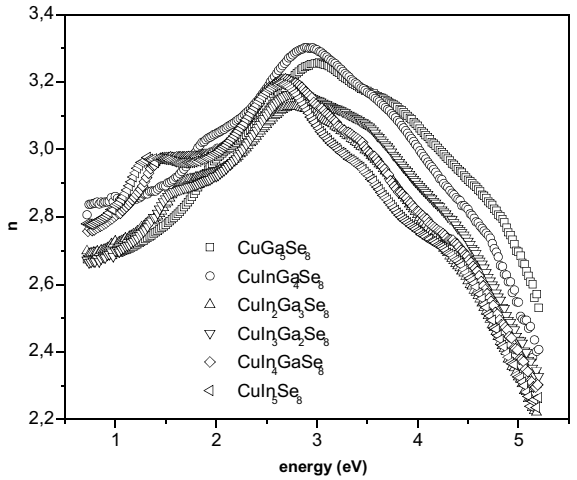

Figure 1. Wavelength dependence of the refractive index *n* of the samples $Cu(In_{1-x}Ga_x)_5Se_8$.

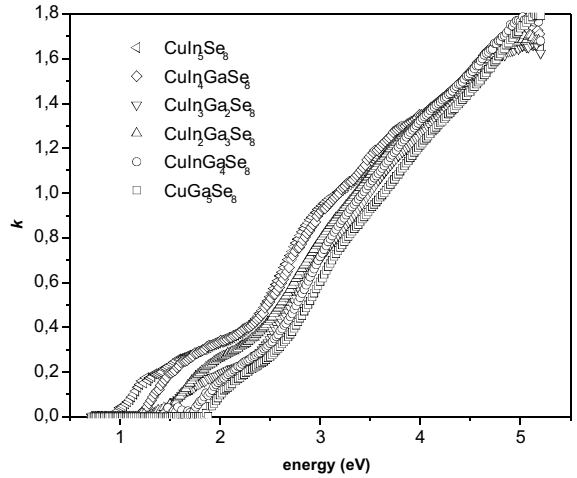

Figure 2. Wavelength dependence of the extinction coefficient *k* of the samples $Cu(In_{1-x}Ga_x)_5Se_8$.

structure. The features observed in $\varepsilon(\omega)$ in the optical range are related to interband transitions originated by large or singular values of the joint valence and conduction density of states. These points of the band structure are also denoted as van Hove singularities or critical points (CP's) (11, 12). Several CP's are observed in the spectra of

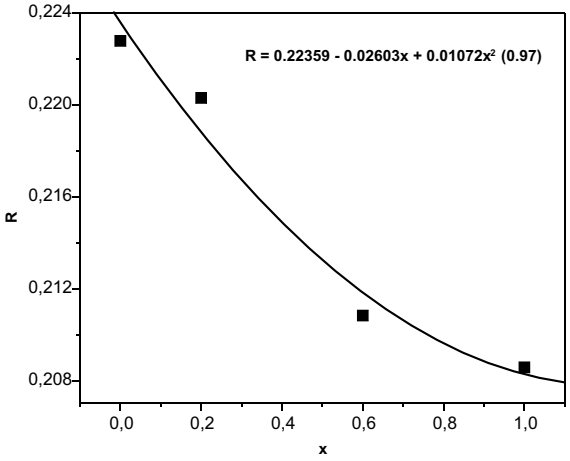

Figure 3. Reflectivity R of $Cu(In_{1-x}Ga_x)_5Se_8$ calculated at the near infrared wavelength of 1.523 μm of the He-Ne laser. R is well fitted as a quadratic function of the alloys composition x.

Figure 1. They can be better resolved in their numerical second derivatives. We calculated derivatives using smoothing polynomials and obtained critical point energies from fitting to standard analytic line shapes (11-14).

The CP's can be analyzed in terms of this standard analytic line shapes:

$$\varepsilon(\omega) = C - Ae^{j\phi}(\omega - E - j\Gamma)^n \qquad [6]$$

The critical-point parameters, amplitude *A*, energy threshold *E*, broadening Γ and excitonic phase ϕ are determined by fitting the numerically obtained second-derivative spectra $d^2\varepsilon(\omega)/d\omega^2$ of the experimental data $\varepsilon(\omega)$ to the relations:

$$\frac{d^2\varepsilon(\omega)}{d\omega^2} = \begin{cases} -n(n-1)Ae^{j\phi}(\omega - E - j\Gamma)^{n-2} & n \neq 0 \\ Ae^{j\phi}(\omega - E - j\Gamma)^{-2} & n = 0 \end{cases} \qquad [7]$$

The exponent n has the value -1/2 for one-dimensional (1D), 0 for 2D and ½ for 3D CP's. Discrete excitons with Lorentzian line shape are represented by n= -1.

The fundamental band gap transitions were fitted only to the real part spectra, and the rest of structure were not considered in

this work because the band structure of these alloys have not been calculated yet inclusive the edges. This reason makes impossible to figure out the meaning of the rest of the structures. Thus, we fitted all compositions following this scheme. For all the samples, the band gap features were best fitted with three-dimensional critical points, $\phi = 0$ and *A* results positive, corresponding our peaks to M1 CP's (11). It is reported that when $\phi = 0$, it represents a pure minimum (14) and corresponds to a Lorentzian line shape (12).

Figures 4-7 shows the second-derivative spectra of the real part of ε for four representative composition of the $Cu(In_{1-x}Ga_x)_5Se_8$ system. Table 2 lists the energy gap values measured by ellipsometry (Eg_e) and by optical absorption (Eg_T) (7) for all studied compositions. The Eg values as a function of x are shown in Figure 8. We observed $Eg_T < Eg_e$ for all compositions. It is also observed that both Eg_T and Eg_e for the end compositions are in good agreement with the values reported by other authors (7, 8, 10, 15-17).

The Eg vs. x data in Figure 8 can be fitted to the relations:

$$Eg_T = 1.17214 + 0.45179\ x + 0.20536\ x^2\ (0.99) \quad [8]$$

$$Eg_e = 1.28064 + 0.58825\ x + 0.11518\ x^2\ (0.99) \quad [9]$$

Also, we report the dielectric constant at high frequency ε_∞ for each composition. They have been determined fitting the real refractive index to the Sellmeier dispersion formula at energies below the gap (18). The Sellmeier formula is given by:

$$n = \sqrt{\frac{1 + (a^2 - 1)\lambda^2)}{\lambda^2 - b}} \quad [10]$$

where λ is the wavelength and $a = \varepsilon_\infty^{1/2}$ and b are the constants to be determined by the fitting process. Table 2 shows the values of ε_∞ obtained by this method. Unlikely, it is impossible to compare with other results because these values are not reported until now, so this is an initial proposal about the system.

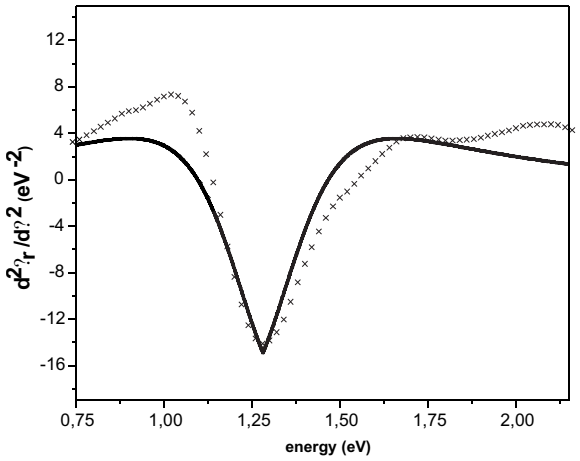

Figure 4. Second-derivative, $d^2\varepsilon_r(\omega)/d\omega^2$, of the real part of e for $CuIn_5Se_8$. Symbol display experimental data and line the results of the fit.

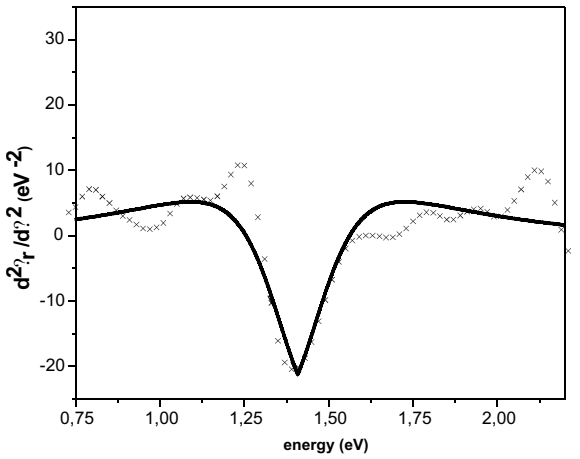

Figure 5. Second-derivative, $d^2\varepsilon_r(\omega)/d\omega^2$, of the real part of ε for $Cu(In_{0.8}Ga_{0.2})_5Se_8$. Symbol display experimental data and line the results of the fit.

The optical absorption coefficient of $Cu(In_{1-x}Ga_x)_5Se_8$ alloys for different values of x, calculated from the equation [3], is shown

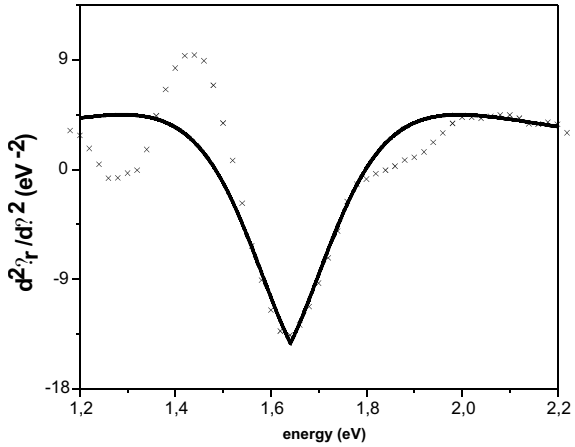

Figure 6. Second-derivative, $d^2\varepsilon_r(\omega)/d\omega^2$,of the real part of ε for $Cu(In_{0.4}Ga_{0.6})_5Se_8$. Symbol display experimental data and line the results of the fit.

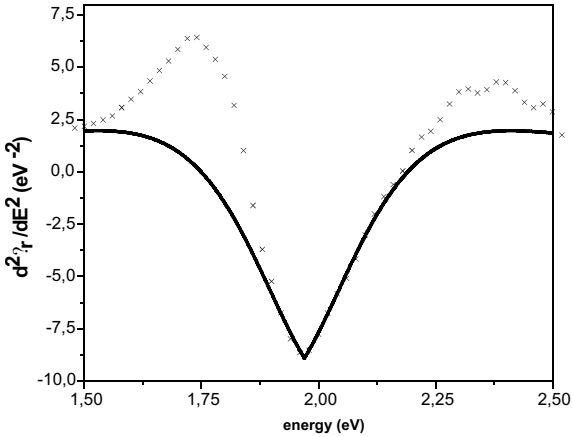

Figure 7. Second-derivative, $d^2\varepsilon_r(\omega)/d\omega^2$,of the real part of e for $CuGa_5Se_8$. Symbol display experimental data and line the results of the fit.

Table 2
Energy gaps of the system $Cu(In_{1-x}Ga_x)5Se_8$ measured by ellipsometry (Eg_e) and optical absorption (Eg_T) [7]. High frequency dielectric constant ε_∞ also shown.

x	Eg_T (eV)	Eg_e (eV)	ε_∞
0	1.17	1.28	7.1893
0.2	1.28	1.41	7.1799
0.4	1.38	1.54	6.7660
0.6	1.50	1.64	6.9542
0.8	1.69	1.86	7.7981
1.0	1.82	1.97	6.8543

as a function of photon energy in Figure 9. It can be observed that α for $CuIn_5Se_8$ (x =0) is about 10^4 cm at roughly 1.18 eV, increases softly with incident energy and is above $8{\cdot}10^5$ cm at 5 eV. Such a high value around the fundamental absorption edge reflects good quality of the samples used in the present work. Similar behavior but with slightly lower values of α can also be noted in Figure 9 near the band edge for other members of the system that have higher x.

Conclusions

Optical properties at room temperature for the $Cu(In_{1-x}Ga_x)_5Se_8$ alloys system, covering the whole composition range, are presented. Special attention has been paid to the problem of minimizing surface effects on the measurements of *n* and *k*, so that the reported values are characteristic of the bulk.

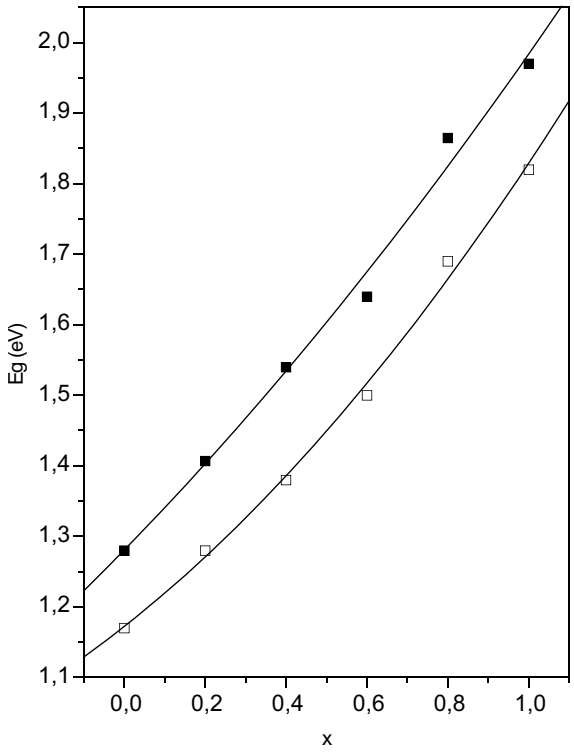

Figure 8. Variation of the energy gap as a function of composition for the $Cu(In_{1-x}Ga_x)_5Se_8$ system. Open squares represent data obtained from optical absorption and full squares represent data from ellipsometry measurements. The solid curves represent the fit according to equations (8) and (9).

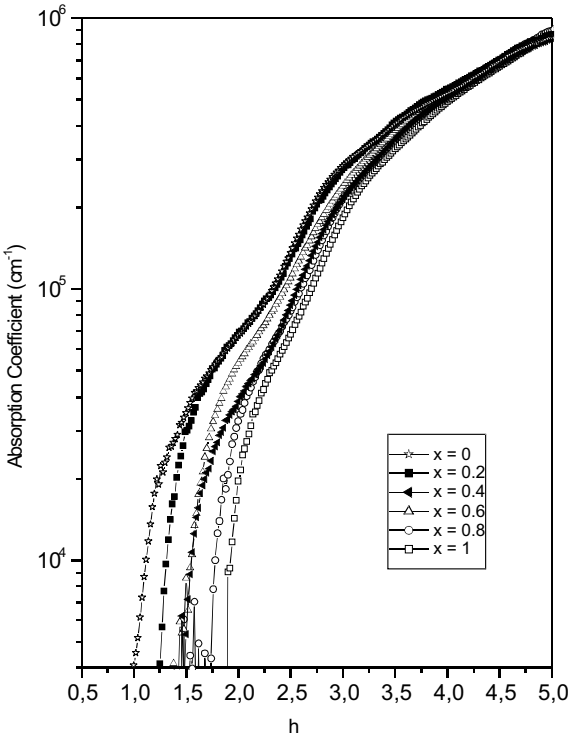

Figure 9. Optical absorption coefficient of $Cu(In_{1-x}Ga_x)_5Se_8$ alloys as a function of incident photon energy between 0.7 and 5.2 eV obtained from ellipsometric data.

From the analysis of the numerical second derivatives of the real part of $\varepsilon(\omega)$, we have obtained the band gap energies for each composition. The energy gap values are in good agreement with those reported by other authors. The calibration curve R(x) at $\lambda = 1.523\ \mu m$ can be applied to determine the alloy composition, for instance, in thin films of these materials, with all the advantages of optical methods. We have reported the dielectric constant at high frequency, ε_∞, for each composition as an initial proposal. The optical absorption coefficient α of $Cu(In_{1-x}Ga_x)_5Se_8$ alloys with different values of x, calculated from the ellipsometric data have shown a high value around the fundamental absorption edge reflecting good quality of the samples used in the present work.

Acknowledgments

This work was supported by grants from FONACIT and CONDES-LUZ.

References

1. ALONSO M.I., GARRIGA M., DURANTE RINCÓN C.A., LEÓN M. ***J Appl Phys*** 88(11): 5796-5801, 2000.
2. DURANTE RINCÓN C.A., HERNÁNDEZ E., ALONSO M.I., GARRIGA M., WASIM S.M.,

RINCÓN C., LEÓN M. ***Mater Chem Phys*** 70(3): 300-304, 2001.

3. ALONSO M.I., GARRIGA M., DURANTE RINCÓN C.A., HERNÁNDEZ E., LEÓN M. ***Appl Phys A*** 74, 659-664, 2002.
4. PAULSON P.D., BIRKMIRE RW., SHAFARMAN W.N. ***J Appl Phys*** 94(2): 879-888, 2003.
5. SEONG G.Y., BANG C.Y., KIM Y.D., WANG J., ASPNES D.E., KOO B.H., YAO T. ***Journal of the Korean Physical Society*** 39: S389-S392, 2001.
6. VEDAM K. ***Thin Solid Films*** 313-314(1-2): 1-9, 1998.
7. DURAN L., WASIM S.M., DURANTE RINCÓN C.A., HERNÁNDEZ E., RINCÓN C., DELGADO L.M., CASTRO J., CONTRERAS J. ***Phys Stat Sol*** (a) 199(2): 220-226, 2003.
8. DURAN L., GUERRERO C., HERNÁNDEZ E., DELGADO J.M., CONTRERAS J., WASIM S.M., DURANTE RINCÓN C.A. ***Journal of Physics and Chemistry of Solids*** 64: 1907-1910, 2003.
9. WASIM S.M., RINCÓN C., MARÍN G., MARQUEZ R., SÁNCHEZ-PEREZ G., GUEVARA R., DELGADO J.M., NIEVES L. ***Materials Research Society, Symposium Proceedings*** 688: H1.2.1-H1.2.6, 2001.
10. REENA PHILIP, R., PRADEEP, B. ***Semicond Sci Technol*** 18: 768-773, 2003.
11. LAUTENSCHLAGER P., GARRIGA M., LOGOTHEDITIS S., CARDONA M. ***Physical Review B*** 35(17): 9174-9189, 1987.
12. LOGOTHEDITIS S., VIÑA L., CARDONA, M. ***Physical Review B*** 31(2): 947-957, 1985.
13. LAUTENSCHLAGER, P., GARRIGA M., Cardona M. ***Physical Review B*** 36(9): 4813-4820, 1987.
14. VIÑA L., HÖCHST H., CARDONA M. ***Physical Review B*** 31(2): 958-967, 1985.
15. WASIM S.M., RINCÓN C., MARÍN G., DELGADO J.M. ***Appl Phys Lett*** 77: 94-96, 2000.
16. RINCÓN C., WASIM S.M., MARÍN G., MÁRQUEZ R., SÁNCHEZ-PEREZ G., NIEVES L. MEDINA E. ***J Appl Phys*** 90(9): 4423-4428, 2001.
17. HERNÁNDEZ E., DURÁN L., DURANTE RINCÓN C.A., ARANGUREN G., GUERRERO C., NARANJO J. ***Cryst Res Technology*** 37(11): 1227-1233, 2002.
18. TATIAN B. ***Appl Optics*** 23: 4477-4481, 1984.